sciendo

Civil and Environmental Engineering
Vol. 18, Issue 2, 641-654, DOI: 10.2478/cee-2022-0059

COMPARISON OF THE EFFICIENCIES OF WEB CUTOUTS FOR STEEL PLATE GIRDERS WITH CORRUGATED WEBS VERSUS FLAT WEBS UNDER PURE SHEAR

A. S. TOHAMY[1,*], Sherif Farouk BADARAN[2] , Ahmed A. EL-SERWI[3], Rabiee Ali SADEEK[4], Amr B. SADDEK[5,6]

[1] Civil Engineering Department, Higher Institute of Engineering and Technology, New Minia, El- Minia, Egypt.
[2] Arab Academy for Science, Technology and Maritime Transport, Branch in Sharjah.
[3] Structural Engineering Departments, Ain Shams University, Egypt.
[4] Civil Engineering Departments, EL-Minia University, Egypt.
[5] Civil Engineering Department, Beni-suef University, Egypt.
[6] Civil Engineering Department, El-Baha University, Kingdom Saudi Arabia.
[*] corresponding author: a.s.tohamy@mhiet.edu.eg

Abstract

Corrugated steel-plate girders are used as structural elements in many applications because of their properties, cutouts are always provided in these plate elements to enable inspection and servicing. This study presents an experimental and analytical study to investigate the efficiency of a steel-plate girder with corrugated webs (GCWs) and flat webs (GFWs) having cutouts under shear loading. In this study, we investigated the influence of some important parameters on the girders' load-bearing capacity. The experimental program was conducted on six full-scale plate girders, which have been tested under central load at mid-span. The analysis was conducted using ANSYS V20 to perform a nonlinear technique for the determination of the ultimate load of the tested girders. Finally, experimental and finite element model were used to define the ratio of increasing carrying capacity in plate girder with flat and corrugated web, having cutout under shear loading. The ultimate strength, failure mechanism, and load-deflection curves from the experimental and analytical study show that the shear capacity of the girder with corrugated web girders extends loads by 22 % compared with the flat web.

Keywords:

Corrugated webs;
Flat webs;
Cutouts;
Shear buckling;
Experimental test.

1 Introduction

Recently, girders with corrugated webs (GCW) represent an economical solution to structural applications than girders with flat webs GFW owing to their high shear-buckling strength. Using corrugated webs instead of flat webs reduces the web thickness, increases the out-of-plane stiffness and buckling strength without any vertical or horizontal stiffeners.

Corrugated webs were first used in aircraft design. Furthermore, it has been used in many megaprojects, such as bridges and multi-stories and industrial buildings Fig. 1. Several studies have focused on steel GCW because it is an excellent load-carrying member, and using thinner thickness webs, it saves from 10 % to 30 % of the cost compared with conventionally fabricated sections. In practical applications, sections with trapezoidal and sinusoidal corrugation profiles are used Fig. 2.

Zhang et al. [1] theoretically explained, using rotated stress-filed method, the shear-failure mechanisms for girders with corrugated steel. They used ANSYS to investigate the post-buckling performance and corresponding ultimate failure mechanism for 24 I-beam specimens. They proved that the girder fails when the plastic hinge forms in the flange. Papangelis [2] used a direct strength

method to compare the obtained results with previous finite element analysis of calculating the capacity factor of beams with corrugated webs under wind load and found that 0.9 is a suitable capacity factor. J. Y. Oh et al. [3] based on the finite element analysis and the mechanical approach confirmed that the accordion effect induced in steel beams with corrugated webs at the prestress transfer was greatly dominated by the geometric characteristics of corrugated webs, and it can be simply quantified using key factors.

Fig. 1: Usage of corrugated steel webs.

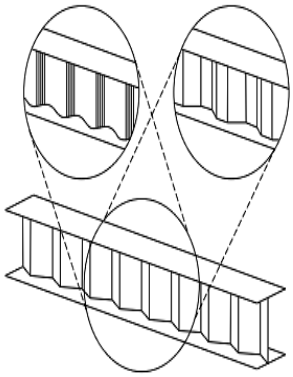

Fig. 2: Beam with sinusoidal, trapezoidal and triangularly corrugated web.

Zubkov et al. [4] investigated the effect on load-bearing capacity for six I-Beams with sinusoidal corrugated web beams under concentrated forces. They found that when the yield strength in the web is achieved, the value of flange tension is 60 % – 90 % and load-bearing capacity is impacted by eccentricity between the axis of webs and flanges.

Cao et al. [5] observed the three failure modes for five welded H-shape steel girder with corrugated webs. The buckling performance for the tested girders were obtained and compared with the ANSYS analytical results, which showed that the capacity owing to shear for corrugated web was 19.4 % for web thickness equal to 3 mm. For competitive studies Bakr et al.[6] focused on the ultimate-strength capacity of plate girders with trapezoidal-corrugated and flat webs, which may reach 60 % for plate girders with corrugated webs having a high slenderness ratio compared with flat webs, while Ezzeldin Yazeed [7] numerically stated that I-girder with corrugated webs have a resistance for lateral tortional buckling, 12 % – 37 % higher, than the GFW, Sachin et al.[8] who found that the maximum shear force obtained in corrugated webs is bigger than that of flat webs with 37 % – 66 %,

For operational reasons in structures of industrial and civil buildings, passing ventilation, water supply, heating, electricity, and other pipelines is necessary, which require making cutouts in the beam webs, and beams with corrugated web present a solution is such cases where cutouts are necessarily see Fig. 3. Hassanein [9] studied the shear behavior of tubular plate girders, with square opening, and compared the results with flat-flange plate girders, with square openings, and a new conclusion were presented.

Lindner et al. [10] investigated girders with trapezoidal corrugated web plates with cutouts; they focused on the local buckling beha0vior of those girders with web openings. Romeijn et al. [11]

presented a basic parametric study for girders with trapezoidal corrugated webs having cutouts, which showed that any increase in the horizontal eccentricity of the cutout lowers the shear resistance. Adel H. Salem et al. [12] used finite element program COSMOS/M to concern the critical shear load of corrugated web girders with wide web openings, the openings in shear panels reduced the critical shear load of corrugated web girders. Finally, an approximate formula for designers has been suggested for practical cases.

The concentration of stresses near the cutout of the web, which can lead to the destruction of the entire structure, is a major challenge. Kudryavtsev [13] studied the stress concentration factors obtained near the circular opening in cases of its location in zone pure and transverse bending of the beam. Recommendations are given for practical design of corrugated web beams weakened by circular openings. While Adewole Kazeem et al. [14] studied fracture failure of double bolt shear out using finite element method.

Fig. 3: Web opening in frames.

Narayanan [15] investigated shear buckling for square plates with different boundary conditions, containing circular or square holes, using the finite element approach. Abdel-Lateef [16] obtained the critical compressive stress for rectangular plates with holes using minimum energy approach.

Samadhan et al. [17] conducted an experimental and parametrical study on steel beams with circular and rectangular web openings, and the results were used to optimize the aspect ratio and spacing to diameter ratio of the openings, where Kiymaz et al. [18] performed a finite element analysis on a series of beam models with sinusoidal corrugation using different corrugation density and relative opening diameters.

In this paper, we represent a comparative study on the ultimate shear capacity for GCWs and GFWs with and without cutouts using experimental and FEM approaches.

2 Experimental investigation

2.1 Laboratory models

Six girder specimens were manufactured by local steel fabricator in welding workshop, and all tests were performed in the steel construction laboratory, Faculty of Engineering, Assuit University.

The first three had GCW and the other three had GFW with and without cutouts. The cutouts are always in the first panel behind the support, although the cutout size is from the centroid of the panel.

2.2 Geometry of models

All girders having web depth of 300 mm, web thickness of 1.5 mm with aspect ratio web height to thickness equals 200, the flange width is 100 mm, and its thickness is 10 mm, and the girder span is 1440 mm. Profiles for girders with corrugated web are shown in Fig. 4 and Table 1. GFW are listed in Table 2 and their profiles are shown in Fig. 5.

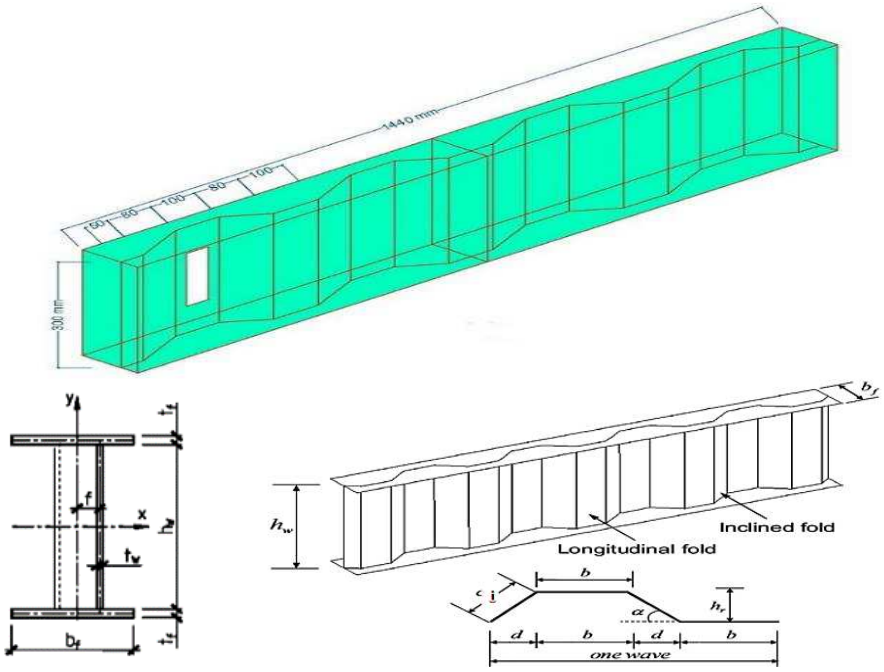

Fig. 4: Dimensions of GCWs.

Three steel-plate stiffeners, 100 mm × 10 mm, were used in GCW1, GCW2, and GCW3: two over the supports and one under the load, however, for GFW1, GFW2, and GFW3, five stiffeners, 100 mm × 10 mm two over the supports, one under the load, and two at quarter span were used. All girders were over hanged, and one load was applied at the mid-span of each girder. Webs in all girders were welded continuously to flanges and vertical stiffeners using filet welds. In addition, stiffener plates have filet weld to the flange plates on two sides. Procedures for welding were followed to avoid web imperfection.

Table 1: Dimensions of girders with corrugated webs.

Model	h_W [mm]	t_W [mm]	b [mm]	d [mm]	h_W / t_W	b/ h_W	Cutout size	α [degree]
GCW 1	300	1.5	100	80	200	0.33	------	37
GCW 2	300	1.5	100	80	200	0.33	15 × 5	37
GCW 3	300	1.5	100	80	200	0.33	2(15 × 5)	37

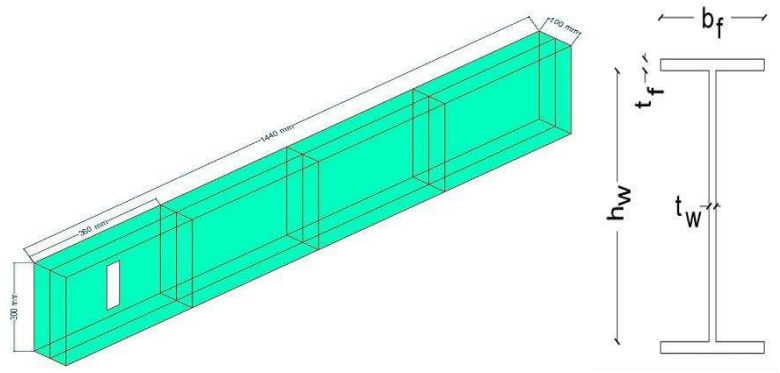

Figure 5: Dimensions of GFWs.

Table 2: Dimensions of girders with flat beams.

Model	h_W [mm]	t_W [mm]	b_f [mm]	t_f [mm]	h_W / t_W	b/ h_W	Cut out size [mm]
GFW 1	300	1.5	100	10	200	1.2	------
GFW 2	300	1.5	100	10	200	1.2	150 x 50
GFW 3	300	1.5	100	10	200	1.2	2(150 x 50)

2.3 Material properties

To obtain mechanical properties required for numerical modeling, such as yield strength, ultimate strength, modulus of elasticity, and elongation of tested materials, six tensile coupons were tested, three from the web and three for the flange, which were cut from the tested specimens.

Tables 3, 4 show the average mechanical properties of the steel used in girders for web and flange under tensile test.

Table 3: Mechanical prop. of web specimens.

Yield strength of web	*Fy* [MPa]	*Fu* [MPa]	*E* [MPa]	Elongation [%]
	262.8	358.9	201000	24

Table 4: Mechanical prop. of flange specimens.

Yield strength of Flange	*Fy* [MPa]	*Fu* [MPa]	*E* [MPa]	Elongation [%]
	281.5	402.1	201000	28

2.4 Test load

In the steel construction laboratory, Faculty of Engineering, Assuit University, simply supported girder, under one concentrated load, which was applied at the mid-span of each girder across the top flange and over the mid-stiffener, as shown in Fig. 6, 7. Fig. 8 represent the two supports for the tested girder, Fig. 9, 10 show the load test for the six tested girders with corrugated and flat webs, respectively. The increasing rate of the load is 0.5 t and it was applied until the beam fails. Linear variable displacement transducers (LVDT) were recorded with computer, as shown in Fig. 11. Visual observations were made during the test. First, for all tests, the loading piston was adjusted to contact the top flange of the distributor beam using suitable number of steel plates.

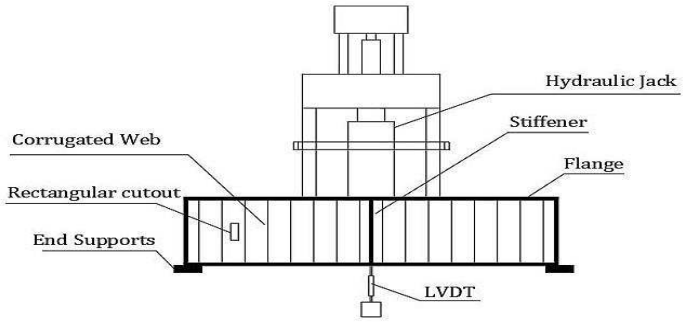

Fig. 6: Schematic view of test setup.

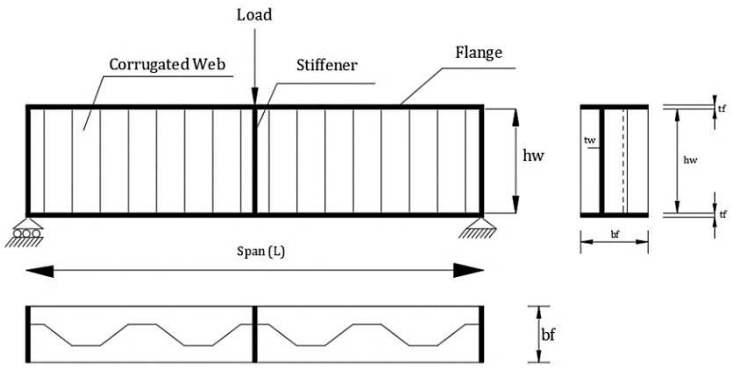

Fig. 7: Load application.

2.5 Test results

Loading of the girders was terminated after the maximum load was attained. Maintaining the load control as the recorded load began to drop was difficult, and ultimate load was reached at the top of load-deflection curve. A full description for girders collapse discussed laterally, the test results are given in Table 7. The load increased to the max capacity at failure, for all tested specimens. The

relationship between the vertical deflection at mid-height of the web and the ultimate load are plotted in Fig 12 for GCW and 13 GFW, respectively.

a) roller support

b) hinged support

Fig. 8: Types of support for tested girders a) roller support, b) hinged support.

Fig. 9: GCW under load test.

Fig. 10: GFW under load test.

Fig. 11: Data logger.

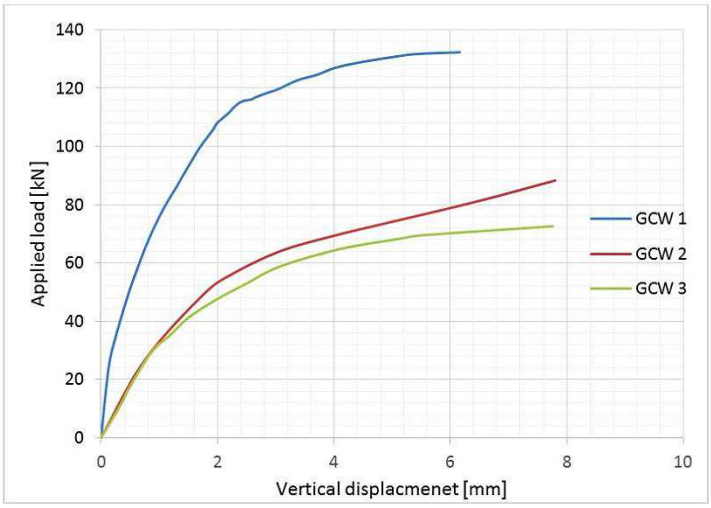

Fig. 12: Applied load versus vertical displacement at mid-span for GCW.

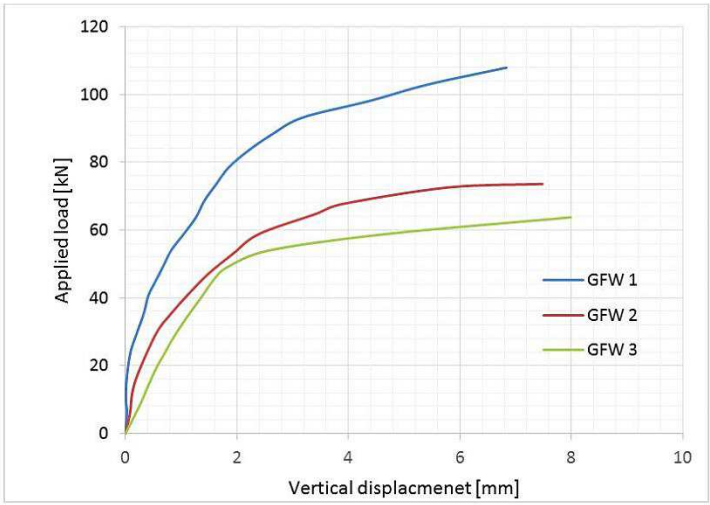

Fig. 13: Applied load versus vertical displacement at mid-span for GFW.

3 Numerical analyses

3.1 Verification of FE Model

The finite element model was validated against the experimental test results of three steel beams with trapezoidally corrugated web listed in Table 5 [19]. Comparison between results of tested beam specimens and fnite element modelling are plotted in Table 6 and Fig. 14. From comparison results, it is concluded that the beams are modelled suitably.

Table 5: Dimensions of tesed beams

Girder No.	b [mm]	d [mm]	h_W [mm]	t_W [mm]	bf [mm]	tf [mm]
BCW (1)	50	40	300	1.5	100	10
BCW (2)	75	60	300	1.5	100	10
BCW (3)	30	24	300	1.5	100	10

Table 6: Experimental and FEM results

Girder No.	τ_y [MPa]	$\tau_{cr,exp}$ [MPa]	$\tau_{cr,FE}$ [MPa]	$\tau_{cr,exp}/\ \tau_{cr,FE}$
BCW (1)	141.45	133.3	135.8	0.982
GCW 2	141.45	120	121.69	0.986
GCW 3	141.45	138. 9	140.44	0.989

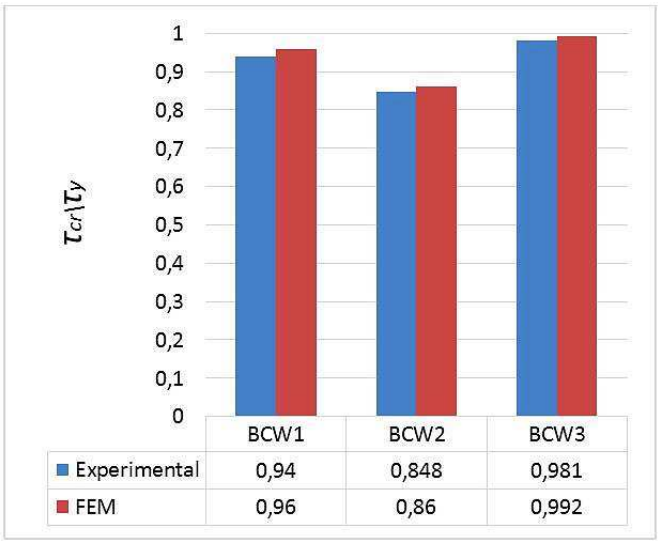

Fig. 14: Comparison between Experimental [19] and FEM.

3.2 Finite element analysis

Finite element analysis (FEA) package, ANSYS /V20 ANSYS Work bench, [20] was used to study the behavior of GCW and GFW of the six tested girder specimens. For members with potential buckling ability, two dependent analyses are required in the FEA. First, the eigenvalue buckling analysis, for obtaining the buckling modes of these members after that a nonlinear analysis, has performed to include geometric and material nonlinearities.

3.3 Modeling setup

Workbench platform working on Multiphysics simulation is easy and employs a tree-like navigation structure to define all parts of their simulation: geometry, engineering data, mesh, loads, boundary conditions and results, Fig. 15.

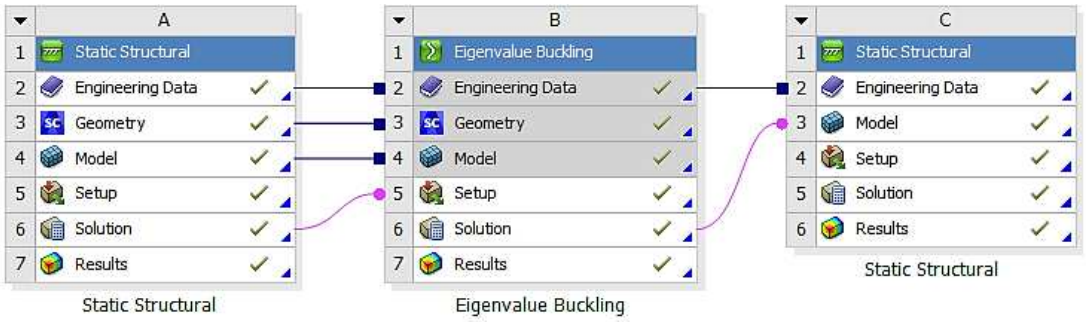

Fig. 15: ANSYS Workbench platform.

We used the same average mechanical properties for both web and flange coupons at the starting stage, Tables 3, 4, after that, a 3-D finite element models were created to simulate the test specimens using the same dimensions for corrugated and flat girders, Tables 1, 2, as shown in Fig. 15a. When in the mechanical application, the model is automatically meshed at solve time and element size equal to 10.0 mm as shown in Fig. 16b.

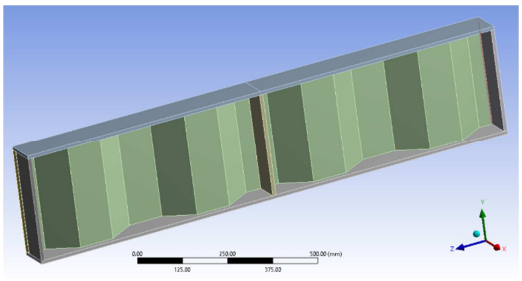

Fig. 16a: 3-D Specimens model.

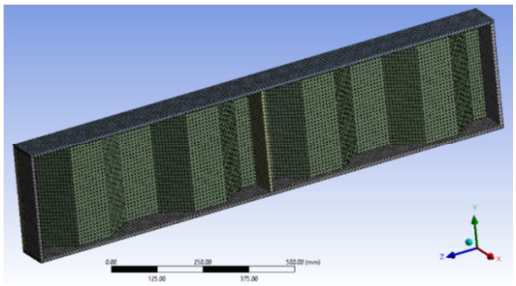

Fig. 16b: Specimens mesh.

The experimental test setup has the configuration of a simply supported beam with one load and boundary conditions, as shown in Fig. 16c, 16d under one concentrated load as shown in Fig. 16e.

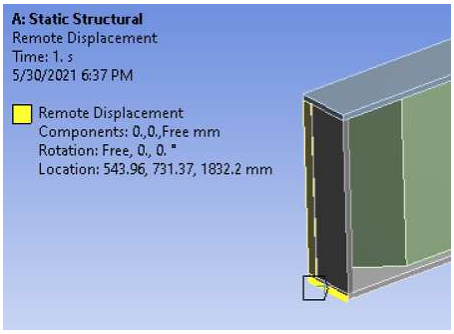

Fig. 16c: Boundary condition for roller support.

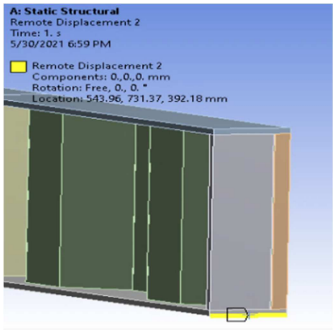

Fig. 16d: Boundary condition for hinged support.

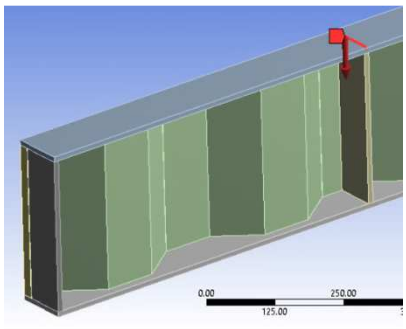

Fig. 16e: Loads on the specimens

3.4 Finite element results

In this section, a series of nonlinear analysis has been used to predict the failure modes, ultimate loads of the tested specimens, and to obtain relations between load and deflection. The ultimate shear capacity from the experimental test and finite element analysis for GCWs and GFWs, comparing the two values, is presented in Table 7. The comparison showed that the solution of the FEM is related to the experimental solution. In addition, the vertical displacement at mid-span of the tested girders, to the applied load, for experimental and analytical studies is plotted in Fig. 17a, b, c, d, e, and f.

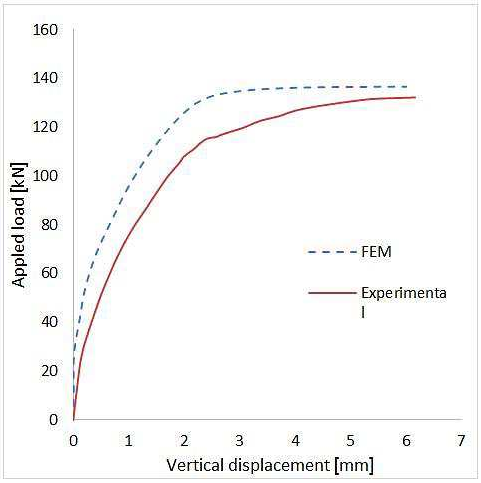

Fig. 17a: Load-deflection curve for GCW1.

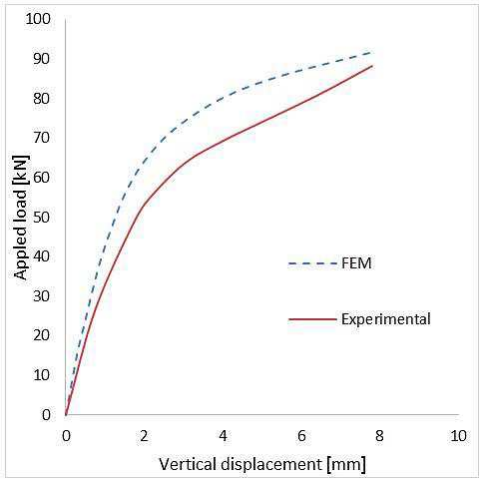

Fig. 17b: Load-deflection curve for GCW2.

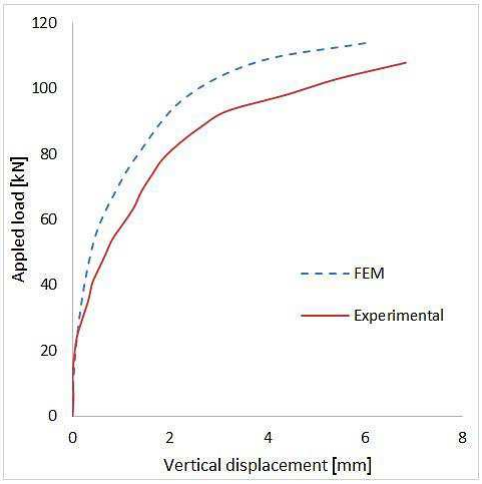

Fig. 17c: Load-deflection curve for GCW3.

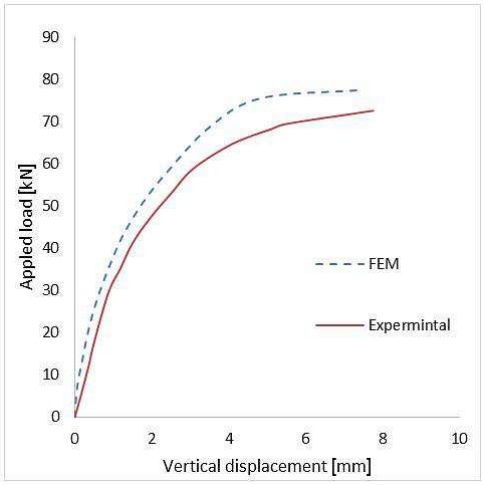

Fig. 17d: Load-deflection curve for GFW1.

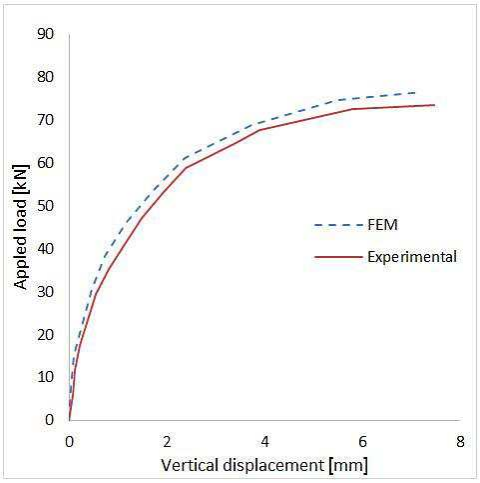

Fig. 17e: Load-deflection curve for GFW2.

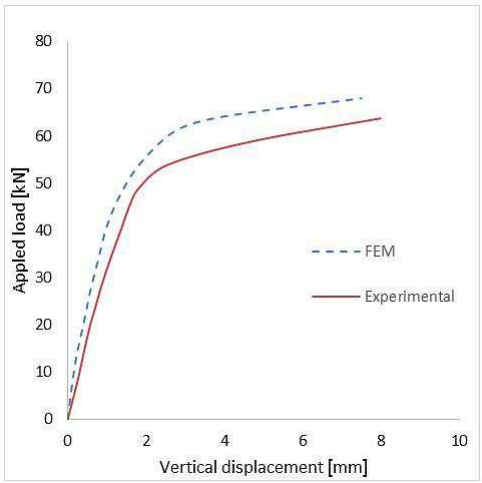

Fig. 17f: Load-deflection curve for GFW3.

3.4 Results and discussion

For all tested girders, the failure occurred owing to the buckling of the web. The deformed shapes of all tested girder specimens are shown in Fig 18a, b, c, d, e, and f. The failure of the six beams was due to buckling of web, which reached its ultimate capacity without any contribution of flanges. In tested beams, the load is increased till buckling initiates at the critical buckling load, then, the load increased until final failure at ultimate load, which was recorded as the load after that stage has an extreme deflection.

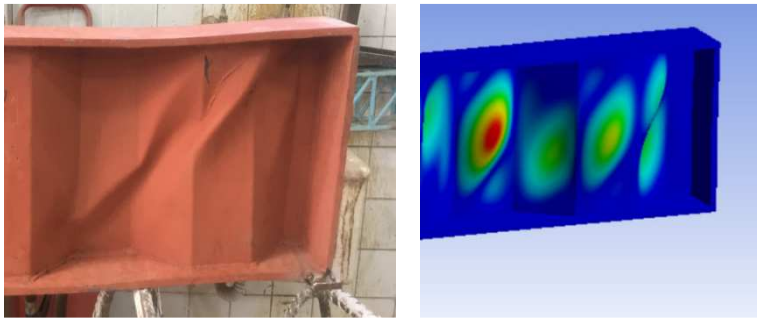

Fig. 18a: Deformed shape for GCW1 EXP. VC FEM.

The deformed shapes for GCW1 (without cutout) shown in Fig. 18a which shows the comparison between experimental and numerical failure pattern for GCW1. Diagonal buckling throughout the entire web (global buckling) was observed in both the experimental and numerical investigations

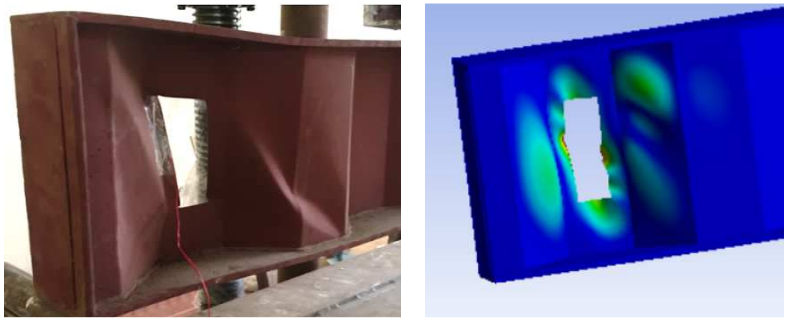

Fig. 18b: Deformed shape for GCW2 EXP. VC FEM.

The deformed shapes for GCW2 (with one cutout) shown in Fig. 18b which shows the comparison between experimental and numerical failure pattern for GCW2. Diagonal buckling throughout the entire web (interactive buckling) was observed in both the experimental and numerical investigations.

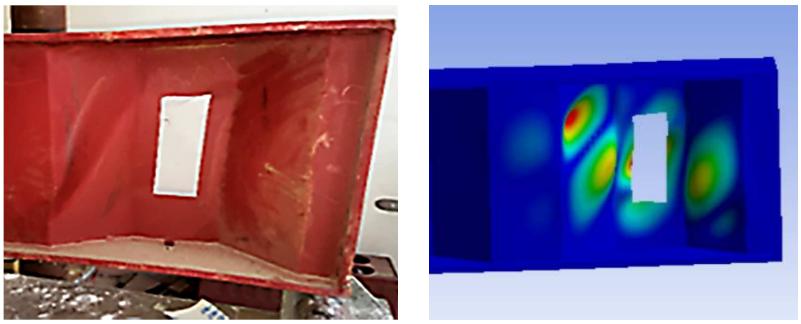

Fig. 18c: Deformed shape for GCW3 EXP. VC FEM.

The deformed shapes for GCW3 (with two cutouts) shown in Fig. 18c, the comparison between experimental and numerical failure pattern shows that diagonal buckling throughout the entire web (interactive buckling) was observed in both the experimental and numerical investigations.

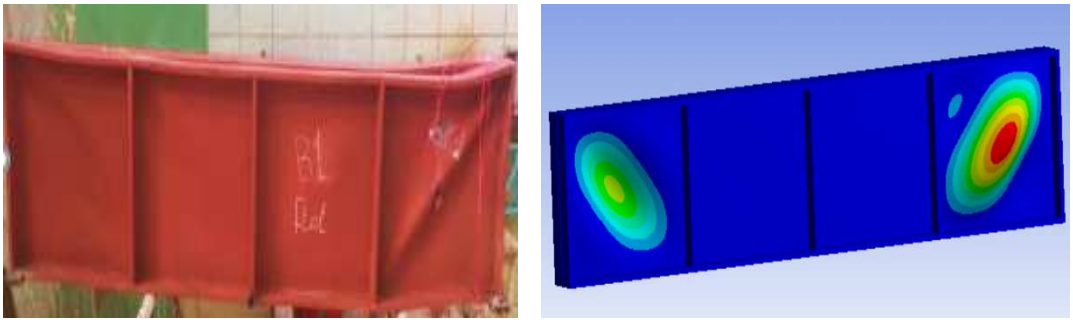

Fig. 18d: Deformed shape for GFW1 EXP. VC FEM.

The comparison between experimental and numerical failure pattern for GFW1 (without cutout) are shown in Fig. 18d.The deformed shows diagonal buckling throughout the entire web (over all buckling) was observed in both the experimental and numerical investigations.

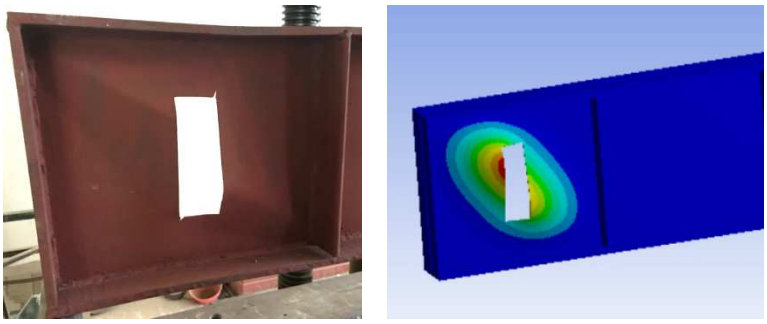

Fig. 18e: Deformed shape for GFW2 EXP. VC FEM.

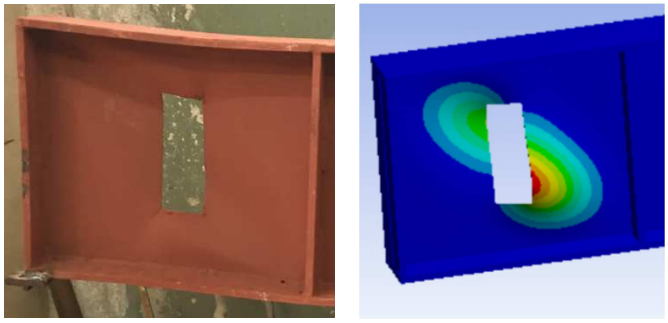

Fig. 18f: Deformed shape for GFW3 EXP. VC FEM.

The comparison between experimental and numerical failure pattern for GFW2 (with one cutout) are shown in Fig. 18e. Deformed shapes for GFW2 shows diagonal buckling throughout the entire web (over all buckling) was observed in both the experimental and numerical investigations.

he comparison between experimental and numerical failure pattern for GFW3 (with two cutouts) are shown in Fig. 18f. Deformed shapes for GFW3 shows diagonal buckling throughout the entire web (over all buckling) was observed in both the experimental and numerical investigations.

Table 7: Experimental and finite element shear load at failure.

Specimens No.	Shear force experimental	Shear force FEM	% difference
GCW1	132.38	136.7	+ 3.2 %
GCW2	88.25	91.68	+ 3.87 %
GCW3	72.56	77.46	+ 6.75 %
GFW1	107.87	113.85	+ 5.6 %
GFW2	73.54	76.48	+ 3.99 %
GFW3	63.74	67.98	+ 6.65 %

Finally, to evaluate the effect of web corrugation and web cutout on the shear capacity, girders with corrugated and flat webs are compared at the same web thickness 1.5 mm. The ratio of web thickness is (1) and the same ratio of web height to web thickness is 200, which is a good comparison from results of experimental and finite element specimens. Figs. 19 – 23 show the girders shearing capacity without using cutouts for GCW1 and GFW1 and after using single and double cutouts for GCW2, GCW3, GCF2, and GFW3.

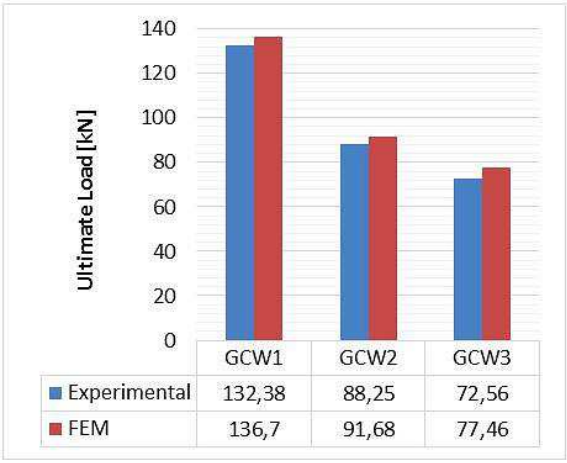

Fig. 19: Results for GCWs.

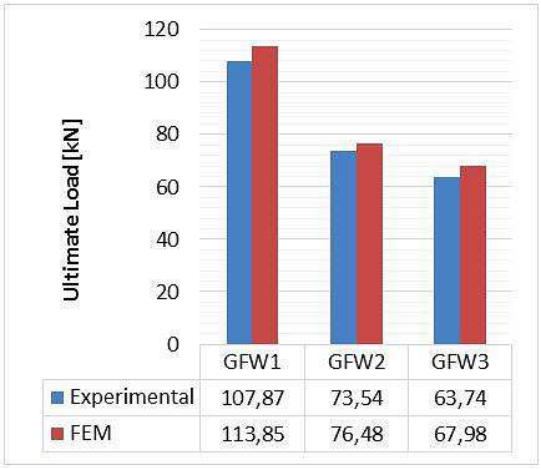

Fig. 20: Results for GFWs.

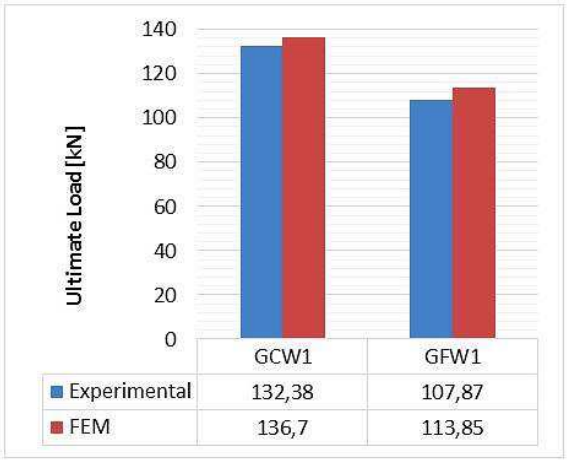

Fig. 21: GCW1 vs GFW1.

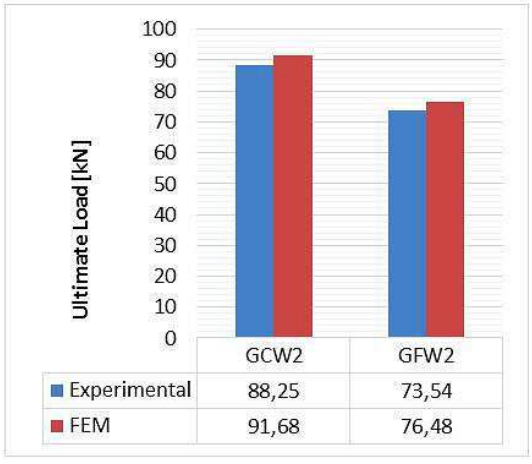

Fig. 22: GCW2 vs GFW2.

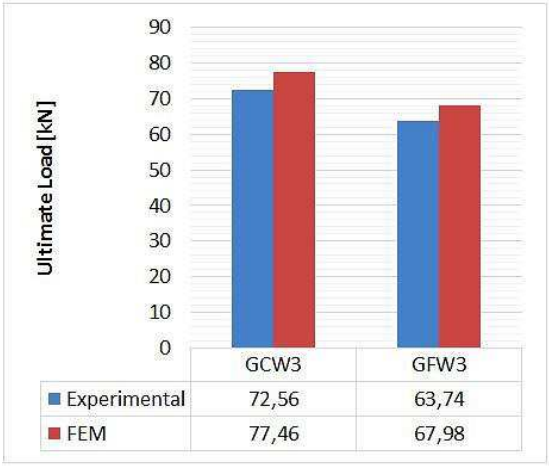

Fig. 23: GCW3 vs GFW3

4 Conclusion discussion

From results and comparison, we arrived at the following conclusion:

1) Experimental results show that the failure of the section occurs owing to the shear buckling of web and distortional buckling around the cutouts.

2) The comparison of experimental and analytical results shows that ANSYS software can predict, with accuracy below 7 %, the ultimate load behavior of the tested specimens, as well as the matching of load-deflection curves.

3) For girders without cutouts and ratio of web thickness 1.0, GCW1 tolerate loads by 22 % more than GFW1.

4) For Girders with one cutout and ratio of web thickness, 1.0, GCW2 have ultimate load that is 20 % more than GFW2, however, for GCW3 the percentage is about 14 % higher than GFW3.

5) The results show that the ultimate load-carrying capacity decreased with the appearance of one or more cutouts.

6) The connection between corrugated web and stiffeners gives efficient joints because of providing point weld at regular intervals.

7) Plate girder with trapezoidal-corrugated web has less deflection, in span and ratio of web thickness, than plate girders with stiffened flat web.

References

[1] ZHANG, B. - YU, J. - CHEN, W. - WANG, H. – XU, J.: Stress states and shear failure mechanisms of girders with corrugated steel webs. Thin Walled Struct., Vol. 157, 2020, 14 p.

[2] PAPANGELIS, J. - TRAHAIR, N. - HANCOCK, G.: Direct strength method for shear capacity of beams with corrugated webs. J Constr Steel Res., Vol. 137, 2017, pp. 152–160.

[3] JAE-YUEL O. - DEUCK HANG LEE - KANG SU KIM: Accordion effect of prestressed steel beams with corrugated webs. Thin-Walled Structures, Vol. 57, 2012, pp. 49–61.

[4] ZUBKOV, V. - LUKIN, A. - ALPATOV, V.: Experimental research of beams with corrugated web. MATEC Web of Conferences Vol. 196, 2018, 6 p.

[5] CAO, Q. I. - JIANG, H. - WANG, H.: Shear behavior of corrugated steel webs in h shape bridge girders. Math Probl Eng., Vol. 2015, 2015, 15 p., https://doi.org/10.1155/2015/796786.

[6] SADEEK, A. B. - TOHAMY, S. - MOHAMED, O. - IBRAHIM, A.: Behavior of plate girder with corrugated steel web subjected to shear loading. International Conference on Advances in Structural and Geotechnical Engineering, ICASGE 2015.

[7] SAYED-AHMED, E. Y.: Design aspects of steel I-girders with corrugated steel webs. Electron J Struct Eng., Vol. 7. 2007, pp. 27-40.

[8] SACHIN, K. G. - SOWJANYA G. V. – MURALIDHAR, N.: Behaviour of Plate Girder with Flat Web and Corrugated Web. Int. J. Struct., Vol. 2, Iss. 1, 2014, pp. 130–136.

[9] HASSANEIN, M. F.: Shear strength of tubular flange plate girders with square web openings. Eng Struct., Vol. 58, 2014, pp. 92–104.

[10] LINDNER, J. - HUANG, B.: Progress in the analysis of beams with trapezoidally corrugated webs. The 17th Czech and Slovak Intern. Conference on Steel Structures and Bridges, 1994, pp. 151–156.

[11] ROMEIJN, A. - SARKHOSH, R. - HOOP, H.: Basic parametric study on corrugated web girders with cut outs. J Constr Steel Res., Vol. 65, 2009, pp. 395–407.
[12] ADEL H. SALEM - MOHAMED A. EL AGHOURY - AHMED A. MATLOUB: Elastic Buckling Of Corrugated Webs with Openings. Twelfth International Colloquium on Structural and Geotechnical Engineering, 2007.
[13] KUDRYAVTSEV, S.: Influence of web openings on bearing capacity of triangularly corrugated web beam. IOP Conf S Mater Sci Eng., Vol. 365, 2018, 9 p.
[14] ADEWOLE KAZEEM KAYODE, LEOPOLD MBEREYAHO: Finite Element Analysis of Double - Bolt Shear-Out Fracture Failure. Civil and Environmental Engineering, Vol. 16, Iss. 2, 2020, pp. 219-228, DOI: 10.2478/cee-2020-0021.
[15] NARAYANAN, R.: Ultimate shear capacity of plate girder with openings in web. Plated steel structures, stability and strength, Chapter 2, 1983, pp. 39–76,
[16] H. TALAAT ABDEL-LATEEF: Buckling of rectangular steel plates with holes. Bulletin of the Faculty of Engineering, Minia University, Vol. 12, 1993.
[17] SAMADHAN G. MORKHADE - LAXMIKANT M. GUPTA: An experimental and parametric study on steel beams with web openings. Int J Adv Struct Eng., Vol. 7, 2015,pp. 249–260.
[18] KIYMAZ, G. - COSKUN, E. - COSGUN, C. - SECKIN, E. Transverse load carrying capacity of sinusoidally corrugated steel web beams with web openings Steel Compos Struct., Vol. 10, Iss. 1, 2010, pp. 69–85.
[19] HISHAM GOMAA KOTB, Shear Buckling Behavior of Plate Girder with Corrugated Webs. Master Thesis. Minia University, 2016.
[20] ANSYS Release 2020 R1, Inc., Canonsburg, 2020.

Appendix 1

According to ECP (Permanent committee for the code of practice. Egyptian Code of Pracitice for Steel Construction and Bridges (Allowable stress Design). Cairo: Housing and Building National Research Center, 2009. Lateral Tortional Buckling is calculated as:

$$L_u = \frac{1380 * A_f * c_b}{d * f_y}, \quad (1)$$

where $c_b = 1.0$ for simply supported beams.

$$d = h - 4t_f = 30 - 4 * 1 = 26 \text{ cm}, \quad (2)$$

$$\mathrm{A_f} = 10 * 1 = 10 \text{ cm}^2, \quad (3)$$

$$f_y = 281.5 \text{ MPa} = 2.871 \ t/\text{cm}^2, \quad (4)$$

$$L_u = \frac{1380 * A_f * c_b}{d * f_y} = \frac{1380 * 10 * 1}{30 * 2.871} = 160.22 \text{ cm}, \quad (5)$$

which is greater than the span of the tested beam 144 cm.